Cyogenic Thermal Conductivity Measurements of Yb:YAG Ceramics*)

Akifumi IWAMOTO[1,2], Aurelien FOUR[3] and Bertrand BAUDOUY[3]

[1)]*National Institute for Fusion Science, National Institutes of Natural Sciences, 322-6 Oroshi, Toki, Gifu 509-5292, Japan*

[2)]*Institute of Laser Engineering, Osaka University, 2-6 Yamadaoka, Suita, Osaka 565-0871, Japan*

[3)]*Université Paris-Saclay, CEA, Département des Accélérateurs, de la Cryogénie et du Magnétisme, Gif-sur-Yvette, 91191, France*

(Received 11 January 2022 / Accepted 15 February 2022)

Thermal conductivity of 9.8 at% Ytterbium-doped Yttrium Aluminum Garnet (Yb:YAG) ceramics has been measured by three systems at Commissariat à l'Énergie Atomique et aux énergies alternatives (CEA Paris-Saclay) and at the National Institute for Fusion Science (NIFS). For accurate measurements, thermal impedances in thermal systems should be negligibly small. However, each system includes some thermal impedance in a heat flow path. This paper describes that thermal conductivity of the 9.8% doped Yb:YAG ceramics and discusses the compensation method for thermal impedance in each system.

Keywords: thermal conductivity, Yb:YAG, cryogenic, steady-state differential method

DOI: 10.1585/pfr.17.2405033

1. Introduction

Ytterbium-doped Yttrium Aluminum Garnet (Yb:YAG) is one of the most promising laser materials for high-energy-power lasers. Cooled Yb:YAG is expected to have advantages of higher thermal shock resistance and higher conversion efficiency. Diode Pumped Solid State Laser (DPSSL) systems with cryogenically cooled Yb:YAG technology have been developed for various applications. Laser output of over hundred joules has been demonstrated [1, 2]. The application to laser fusion experiments requires the highest laser power. In the conceptual design of the KOYO-F laser fusion reactor [3,4], cryogenically cooled Yb:YAG lasers are planned to serve as compression and heating lasers with the amount of 1.2 MJ at an operation rate of 16 Hz. More than 90% extraction efficiency would be expected by cooling the Yb:YAG below 200 K. To achieve high repetition rate, the thermal shock resistance of Yb:YAG must be considered. Therefore, thermal conductivity is one of the important properties.

At the beginning of Yb:YAG laser developments, crystal blocks were used because of the requirement of a transparent material and high laser performance. To understand the cryogenic feasibility, thermo-optic properties have been measured in a cryogenic environment [5]. The thermal conductivity of an Yb:YAG crystal depends on the doping ratio of Yb, and a higher Yb doping ratio makes the thermal conductivity lower. The thermal conductivity of Yb:YAG monotonically increases in a temperature range of 300 - 100 K as the temperature decreases. Then transparent Yb:YAG ceramics have been successfully fabricated. The performance of the ceramics has been proved to surpass that of a single crystal [6]. To discuss the difference between a crystal and ceramics, measurements of YAG ceramics have been conducted in cryogenic environment [7,8]. In terms of Yb:YAG ceramics, the thermal conductivity below 100 K measured at the National Institute for Fusion Science (NIFS) has been published [9]. However, no other measurement has yet been published. We report measurements below 100 K as a sequel.

Thermal conductivity, k, has been measured by various thermal systems at many institutes. In general, either a method of a transient heat pulse or a steady state differential one is employed. In the transient heat pulse method, thermal diffusivity, a, is directly evaluated, then thermal conductivity is calculated by the relation of $k = ac\rho$, where c and ρ are the specific heat and the density, respectively. To calculate thermal conductivity, information on c and ρ is required with high accuracy. The transient heat pulse method has the advantage of dealing with small sample sizes. On the other hand, a steady state differential method directly measures thermal conductivity. The thermal conductivity is given by Fourier law's, $q = -k \cdot dT/dx$, where q is the heat flux going through the sample to be tested, and dT is the temperature difference generated by the heat flow through the sample. Therefore, the steady state differential method is expected to measure thermal conductivity with higher accuracy rather than the transient pulse heat method. We chose the steady state differential method.

author's e-mail: iwamoto.akifumi@nifs.ac.jp

*) This article is based on the presentation at the 30th International Toki Conference on Plasma and Fusion Research (ITC30).

In order to realize accurate thermal conductivity measurements, a high accuracy on the measurement of dT generated by a heat flow is essential. Therefore, any thermal impedances due to contact, grease and other non-target materials should be prevented in the dT measurement. However, the immoderate pursuit of accuracy makes a measurement system impractical.

Various experimental systems have been supplied for thermal conductivity measurements at cryogenic temperatures [7, 10–12]. A lot of effort has been made to minimize the uncertainty. To minimize thermal impedances along the heat flow path, the knife edge technique, which is described in reference 7, was applied to measure temperature. The knife edge of a copper (Cu) block with an embedded temperature sensor contacts the sample surface. Temperature can be measured with less uncertainty when heat leak to the temperature sensor via wires is minimized. However, the knife edge technique requires high skill to avoid thermal impedance at the interface. An easy way to attach temperature sensors on a sample was shown in reference 12. Sensors were glued on a sample surface. Heat leak to the sensors via wires must cause an incorrect temperature measurement because high thermal impedance of the glue prevents equalizing the temperature of the sensor itself with the sample surface. For easy temperature measurements, the Cu blocks embedded with temperature sensors are attached to both ends of a sample by mechanical clamps or an adhesive [10, 11]. However, the thermal system includes thermal impedances within a heat flow pass. Therefore, dedicated compensation methods for the thermal impedances must be established for the thermal system. Successful compensation for a thermal impedance caused by an adhesive has been established [11]. The thermal conductivity of 304-series stainless steel was measured. By applying the compensation method, evaluated values are consistent with those from Cryocomp (ver.3.06, Cryodata Inc.). However, thermal contract differential among a sample, an adhesive and Cu might result in the destruction of the adhesive. On the other hand, the mechanical clump technique has the advantage of holding a sample in a cryogenic environment without the thermal contract differential problem. However, the compensation method for the thermal impedance has not been established due to a complicated heat flow path.

Each experimental system must produce the same thermal conductivity curve without system dependence. Alternative experimental systems allow us to measure thermal conductivity of materials with a variety of sizes and shapes. In this study, we select three systems at Commissariat à l'Énergie Atomique et aux énergies alternatives (CEA Paris-Saclay) and NIFS. Also, the thermal conductivity of Yb:YAG ceramics was measured. Then thermal conductivity curves of Yb:YAG ceramics produced from the systems were compared. Compensation for thermal impedances was discussed.

Fig. 1 Picture of the 15 mm long 9.8 at% Yb:YAG ceramics block.

Table 1 Dimensions of the Yb:YAG blocks (mm).

Sample Type	10	15	20
Length	10.017 ±0.002	15.018 ±0.001	20.037 ±0.001
Width	5.063 ±0.003	5.067 ±0.001	5.060 ±0.005
Height	5.016 ±0.002	5.018 ±0.003	5.013 ±0.002

2. Yb:YAG Ceramics Samples

Blocks of 9.8 at% doped Yb:YAG ceramics were prepared with three different lengths. The blocks were produced by Konoshima Chemical Co., Ltd. A picture of the 15 mm long block is represented in Fig. 1. Blocks with a $5 \times 5\,\mathrm{mm}^2$ cross-section and 10 mm, 15 mm or 20 mm lengths were cut from a ceramic bulk. The dimensions of the blocks were measured with a micrometer with 0.001 mm of graduations prior to the tests and are listed in Table 1. The values of width, height and length represented in the table are an average of three points, respectively.

3. Thermal Systems for Thermal Conductivity Measurements

The thermal conductivity of the blocks of Yb:YAG ceramics was measured with three different systems at CEA Paris-Saclay and at NIFS. A measurement system with a 4 K GM cryocooler is possessed by CEA Paris-Saclay, and two kinds of sample holders cooled by a 10 K GM cryocooler are available at NIFS.

3.1 Method of thermal conductivity measurement

The thermal conductivity was measured by the so-called a steady-state differential method. The dimensions in width and height of the Yb:YAG blocks were sufficiently large to consider thermal conduction one-dimensionally within these blocks (see Table 1). Then thermal radiation and convection was carefully reduced to be negligible when compared to conduction. The Fourier law was used to construct an average thermal conductivity over the temperature difference created by the heat flux. This average thermal conductivity, $\overline{k(T)}$ is written as

$$\overline{k(T)} = \frac{1}{T_h - T_c} \int_{T_c}^{T_h} k(T)\mathrm{d}T = \frac{Q}{T_h - T_c} \frac{l}{S}, \qquad (1)$$

when the cross-sectional area, S, is constant over the flux line between two temperatures, T_c (cold side) and T_h (hot side), separated by length l. Q is the applied heat that creates the temperature difference $\Delta T = T_h - T_c$ over l. When presenting the results, the average thermal conductivity is associated with the average temperature over T_h to T_c, because it is easier to compute. This constitutes a systematic error that tends to zero when ΔT tends to zero. In our measurements, we have set Q to have sufficiently small ΔT to neglect this systematic error over the entire range of measurements.

3.2 Thermal conductivity measurement at CEA Paris-Saclay

The 15 mm length Yb:YAG block was employed. Figure 2 shows the schematic of the CEA Paris-Saclay system [10]. Both ends of the block were mechanically clamped by Cu holders: Cu holder 1 and Cu holder 2, which were made of Oxygen Free Copper (OFC), and therefore, the effective length for thermal conductivity measurements became 8.63 mm. To make sure of thermal contact, vacuum grease (Rhodia Silicone Italia S.p.A.) mixed with Cu fine powder (Goodfellow Cambridge Limited), whose maximum particle size was 50 μm was spread on the Cu surface facing the block. The volume fraction, V_f of the Cu powder was around 50% at a rough estimate. V_f was defined as the volume of Cu powder divided by the volume of vacuum grease mixed with Cu powder. The steady-state heat generated by Heater 2 flowed through the Yb:YAG ceramics block via the Cu holders. Two Cernox® sensors were embedded in the holders and measured the temperature difference between the holders. Thermal conduction via the grease charged with Cu powder and the Cu holders, resulted in an extra temperature difference. Heater 1 was attached to Cu holder 1, which was cooled by a 4.2 K Gifford-McMahon (GM) cryocooler (Sumitomo Heavy Industries, Ltd.), to control the whole temperature system. The system was covered by a thermal shield that was cooled by the second stage of the 4.2 K GM cryocooler.

Figure 3 shows the thermal system. Heater 2 generates heat which flows from Cu holder 2 to Cu holder 1 via the

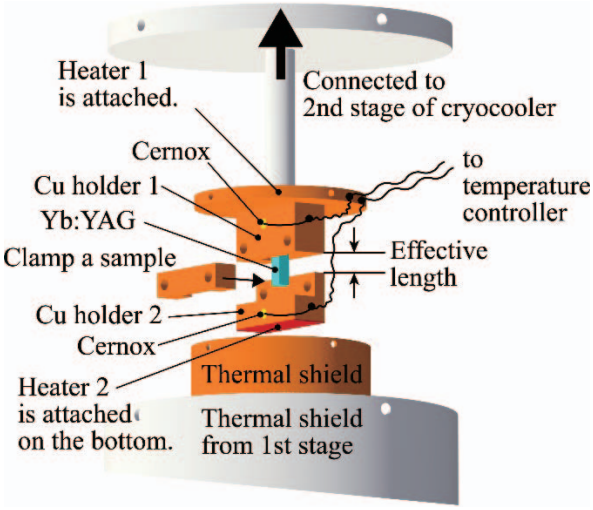

Fig. 2 Schematics of the thermal measurement rig at CEA Paris-Saclay. A film heater as Heater 2 was attached to the bottom of Cu holder 2.

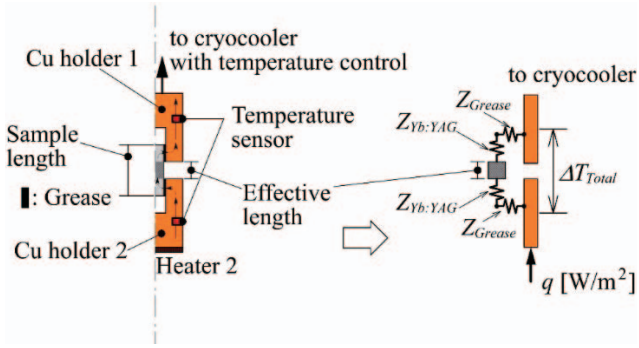

Fig. 3 CEA Paris-Saclay thermal system with the sample and Cu holders. Z_{Grease} and $Z_{Yb:YAG}$ are the thermal impedances of the grease charged with Cu powder and by the non-effective length of the Yb:YAG block, respectively. The temperature difference: ΔT_{Total} are measured by two temperature sensors.

sample block. Cu holder 1 is connected to the cryocooler with temperature control. We could measure the temperature difference between the two holders. Therefore, thermal impedances of a part of the Yb:YAG ceramics block, $Z_{Yb:YAG}$ and the grease, Z_{Grease} must be considered for the evaluation of the intrinsic thermal conductivity of Yb:YAG ceramics.

3.3 Thermal conductivity measurement at NIFS

Two systems: System 1 and System 2, were employed at NIFS. The same 20 K GM cryocooler (Aisin Seiki Co., LTD.) was used. The two systems were attached to the second stage of the cryocooler.

3.3.1 NIFS System 1

The Yb:YAG ceramics blocks of 10 mm, 15 mm and

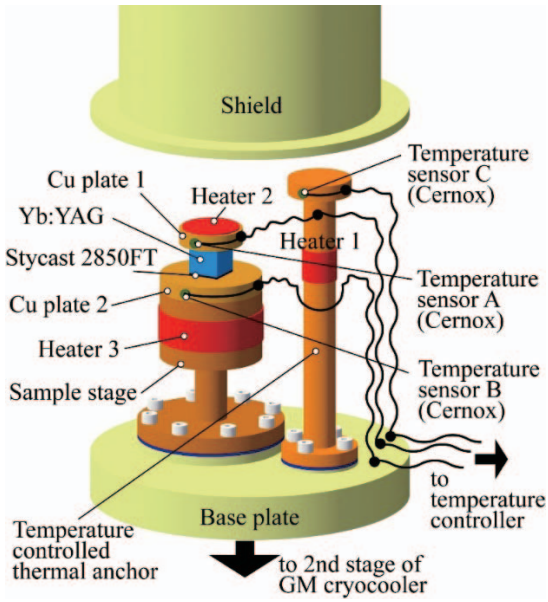

Fig. 4 NIFS System 1. A nichrome wire was used as Heater 1 and Heater 3. A film heater as Heater 2 generated a uniform heat flow through the Yb:YAG ceramics block. A base plate was placed on the second stage of the 20 K GM cryocooler (Aisin Seiki Co., LTD.).

20 mm in length were used. Figure 4 shows the schematic of System 1 [11]. To apply the information in reference 11, both ends of the Yb:YAG ceramics block were glued to Cu plates by Stycast 2850FT, and the same preparation process was employed. The thickness of the Stycast layer was controlled. In curing of the Stycast, the Cu plates were pressed on both ends of the Yb:YAG ceramics block at 39 kPa. Heater 3 controls the whole sample temperature within several mK, and Heater 2 generates the steady state heat flow through the Yb:YAG ceramics block. The temperature difference between both ends of the Yb:YAG ceramics block was measured by Temperature sensors A and B, embedded in Cu plates 1 and 2, which were made of OFC (RRR = 80±20), respectively. Wires to Temperature sensors A and Heater 2 were connected to a temperature controller, Model 350 (Lake Shore Cryogenics, Inc.) via a temperature controlled thermal anchor to reduce heat leak. The thermal anchor was controlled at the same temperature as Cu plate 1 by Heater 1. For this system, possible samples might be limited to glue friendly materials. To reduce the radiation from room temperature, a shield made of OFC was plated with gold.

Figure 5 shows the thermal system. The heat generated by Heater 2 flows down to Cu plate 2 via the Yb:YAG ceramics block. The temperature difference, inclusive of the thermal impedance of the Stycast 2850FT, $Z_{Stycast}$, was measured with the two Cernox® sensors. We have already established the compensation method for the thermal impedance [11]. The thermal conductivity of Yb:YAG ceramics, $k_{Yb:YAG}$ and $Z_{Stycast}$ are calculated as follows,

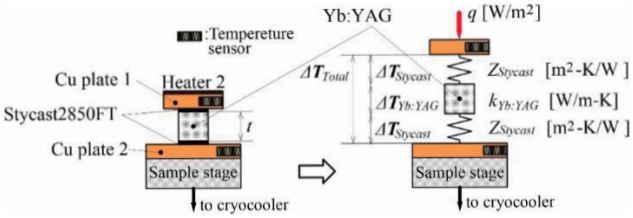

Fig. 5 Thermal system of NIFS System 1 with the Yb:YAG ceramics block and Cu plates.

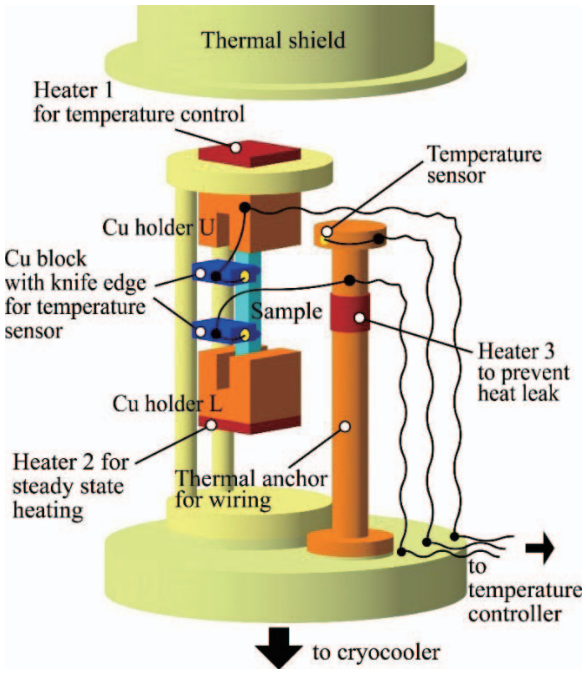

Fig. 6 NIFS System 2. Thermal impedance was eliminated by the knife edge technique for temperature measurements. A base plate was placed on the second stage of the 20 K GM cryocooler (Aisin Seiki Co., LTD.).

$$k_{Yb:YAG} = \frac{t_1 - t_2}{\frac{\Delta T_{Total\,1}}{q_1} - \frac{\Delta T_{Total\,2}}{q_2}}, \tag{2}$$

$$Z_{Stycast} = \frac{t_1 \frac{\Delta T_{Total\,2}}{q_2} - t_2 \frac{\Delta T_{Total\,1}}{q_1}}{2 \cdot (t_1 - t_2)}, \tag{3}$$

where t, q, dT_{Total}, $dT_{Stycast}$ and $dT_{Yb:YAG}$ are the length of the Yb:YAG ceramics block, heat flux, the measured temperature difference with two temperature sensors, temperature differences at the Stycast layer and the Yb:YAG ceramics block, respectively. Here measurements from two samples with different thicknesses: t_1 and t_2 are applied. The subscripts 1 and 2 refer to any two Yb:YAG ceramics blocks. The copper plates made of OFC have much higher thermal conductivity than other materials and can be assumed to be isothermal.

3.3.2 NIFS System 2

The Yb:YAG ceramics block with a 15 mm length was used. Figure 6 shows System 2 at NIFS. Both ends of a

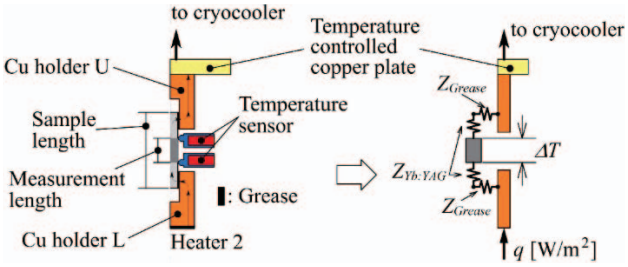

Fig. 7 Thermal system of NIFS System 2.

Yb:YAG ceramics block were pinched in Cu holders. To make a good thermal contact, Cry-Con thermal conductive grease (Lake Shore Cryogenics, Inc.) was spread on Cu surfaces. This sample holding system has the advantage of being able to hold any solid materials down to a cryogenic environment. Heater 1 controls the whole sample temperature within a few mK, and Heater 2 generates the steady-state heat flow through the Yb:YAG ceramics block. For temperature measurements, Cernox® sensors embedded in Cu blocks with a knife-edge were used. The knife-edge can realize line thermal contact with the sample surface, and therefore the distance for the temperature differential can be assigned with a small installation error. However, heat leak to the sensor via wires causes uncertainty, because the line thermal contact at the knife edge makes the temperature gap adverse. Therefore, wires to the Cu blocks were connected to a temperature controller via a temperature controlled thermal anchor. Heater 3 controlled the temperature of the thermal anchor to be the same within several mK as that of Copper holder L. To reduce the radiation from room temperature, the gold-plated shield was installed. Cu blocks and the thermal shield were made of OFC.

Figure 7 shows the thermal arrangement of System 2. The heat generated by Heater 2 at the bottom of Cu holder L flows to Cu holder U via the Yb:YAG ceramics block. According to the system configuration, no thermal impedance ideally affects the ΔT measurement.

4. Results at CEA Paris-Saclay and NIFS

Round-robin thermal conductivity measurements of the Yb:YAG ceramics blocks were conducted at CEA Paris-Saclay and NIFS. Figure 8 shows the thermal conductivity measured at CEA Paris-Saclay and NIFS without any compensations. Error bars represent uncertainties from temperature and heat flux measurements.

Measurements down to 4.2 K were completed without any problem at CEA Paris-Saclay. A mechanical advantage was proved. The curve from CEA Paris-Saclay was lower than those from NIFS, however it looks as if the curve just shifted lower. The discrepancy might be caused by the different types of thermal impedance mentioned above. Using NIFS System 1, measurements could be conducted from 260 K down to 180.6 K, 100.6 K and 70.5 K, using the blocks of 20 mm, 15 mm and 10 mm in length, respectively. A fracture of Stycast 2850FT as the glue made cryogenic measurements impossible. The thermal contract differential among Cu, Styacast 2850FT and Yb:YAG ceramics fractured the Stycast 2850FT layer. Our apprehension on the mechanical weakness of the adhesive was proved to be true. NIFS System 2 produced the highest thermal conductivity profile, as compared to others, because no thermal impedance existed. Measurements from 250.3 K to 11.2 K succeeded. The lower temperature was limited by the cooling capacity of the cryocooler.

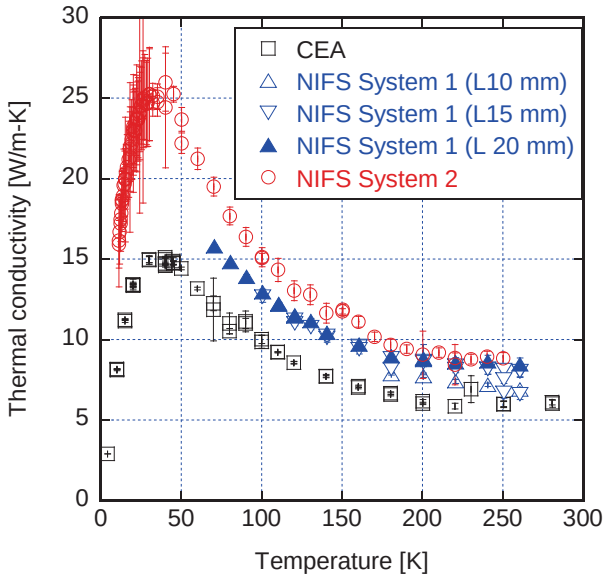

Fig. 8 Thermal conductivity measurements of 9.8 at% Yb:YAG ceramics without any compensations. The data from NIFS System 1 have been published partially in reference [9].

5. Discussions

According to the experimental results, the thermal impedances must affect the accuracy. We should establish compensation methods for the thermal impedances in the systems.

5.1 Compensation for the thermal impedance in NIFS System 1

Applying equations 2 and 3, the thermal conductivity of the Yb:YAG ceramics and the thermal impedance of the Stycast 2850FT layer are calculated from measurements of the Yb:YAG blocks, 15 mm and 20 mm in length. Figures 9 and 10 show the compensated thermal conductivity of Yb:YAG ceramics and the revealed thermal impedance at the Stycast2850FT layer, respectively. The compensated thermal conductivity of the Yb:YAG ceramics well agrees with the measurements of NIFS System 2. The revealed thermal impedances of the Stycast 2850FT layer,

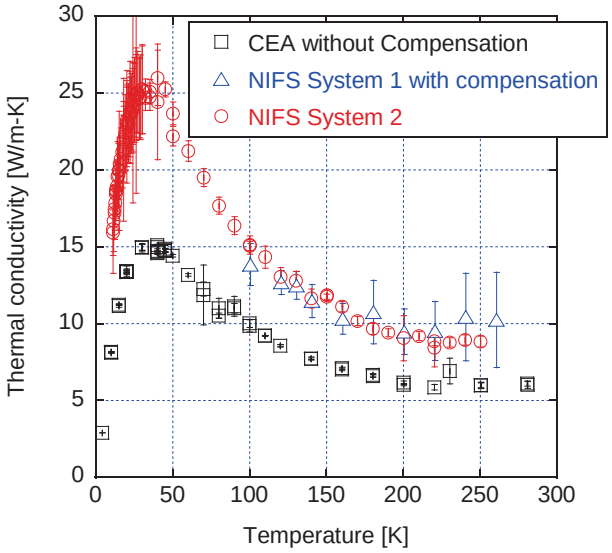

Fig. 9 Compensated thermal conductivity of 9.8 at% Yb:YAG ceramics by equation 2.

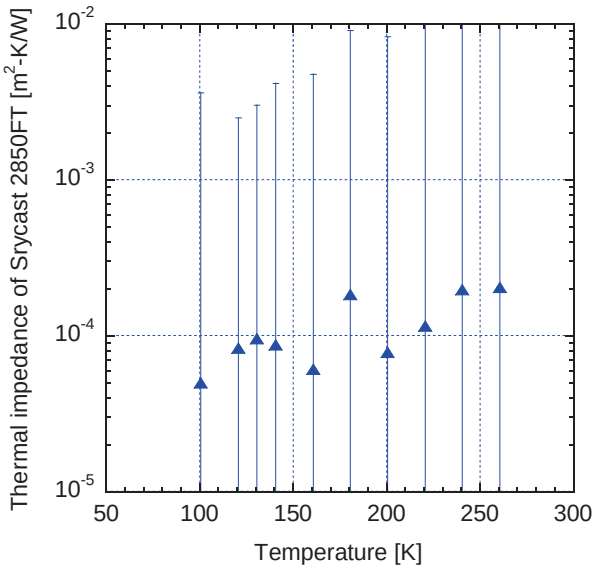

Fig. 10 Revealed thermal impedance at the Stycast 2850FT layer by equation 3.

~0.0001 K-m^2/W, in the 100 to 260 K temperature range are consistent with those in references 11, 13 and 14. Judging from this, the intrinsic thermal conductivity of the Yb:YAG ceramics should be successfully calculated by equation 2. It means NIFS System 2 can itself evaluate the thermal conductivity of Yb:YAG ceramics.

5.2 ANSYS simulation of CEA Paris-Saclay measurement

Values of the thermal conductivity measured at CEA Paris-Saclay are lower than those at NIFS. The discrepancy must come from the thermal impedance at the layer of the mixture of Cu powder and grease in the CEA Paris-Saclay

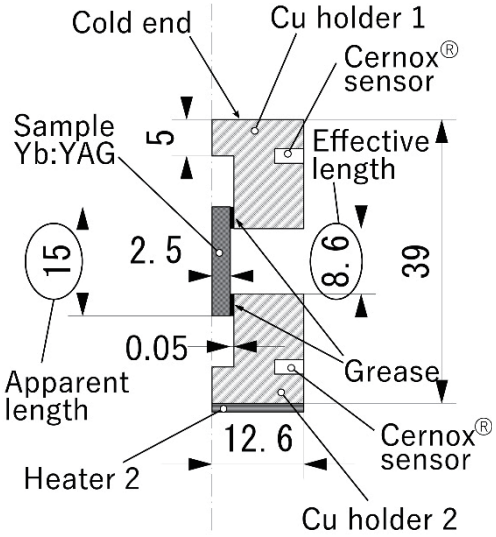

Fig. 11 Plane symmetric 2D model of the Yb:YAG ceramics block and Cu holders in the CEA Paris-Saclay system. Effective sample length is 8.6 mm. In the CEA Paris-Saclay system, the heat which is generated by Heater 2 at the bottom of Cu holder 1 is transferred from the Cu holder to a Yb:YAG ceramics block via the mixture of Cu powder and grease and then flows through the Yb:YAG ceramics block of 15 mm apparent length. The temperature difference measured between the two Cernox® sensors arises from the heat flow path.

system. Both thermal conductivities of the Cu powder and the vacuum grease have not been published in all temperature ranges. Therefore, we try to estimate the thermal conductivity of the mixture from simulation. Then we discuss the ability of the CEA Paris-Saclay system to measure thermal conductivity with high accuracy.

The ANSYS code was used to conduct the thermal analysis of the CEA Paris-Saclay system. The Yb:YAG ceramics block, the Cu holders and the layers of grease charged with Cu powder were modeled. A two dimensional (2D) model of the CEA Paris-Saclay system is shown in Fig. 11. The temperature difference between the Cu holders, which includes temperature drops at the grease layers and at both redundant ends of the Yb:YAG ceramics block, was measured by two Cernox® sensors. We have the measured values on the temperature difference by two Cernox® sensors and on the heat flux through the Yb:YAG ceramics block. We assume that the Cu holders made of OFC had uniform temperature. The thermal conductivity of the Yb:YAG ceramics block measured by NIFS System 2 was used in the model. The thermal conductivity of the mixture of Cu powder and grease is unknown. Heat applied in the experiment was assigned to the heater. While varying the thermal conductivity of the mixture of Cu powder and grease, the temperature difference between Cu holder 1 and 2 were calculated. We found the thermal conductivity of the mixture of Cu powder and grease to be that the temperature difference converged into a measured

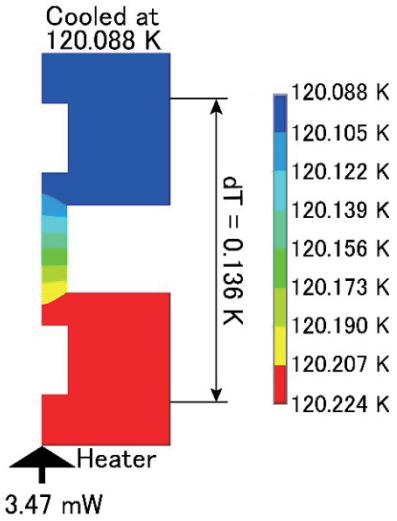

Fig. 12 Example of ANSYS calculation to extract thermal conductivity of the grease. The thermal conductivity of the composite grease is assumed to be 0.775 W/m.K.

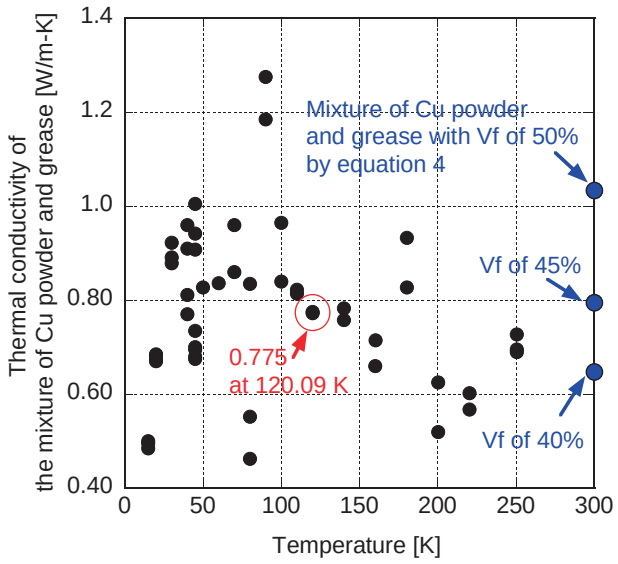

Fig. 13 Thermal conductivity of the mixture of Cu powder and grease estimated by ANSYS calculations.

value by iteration. Eventually the thermal conductivity of the mixture of Cu powder and grease was obtained.

A temperature profile predicted by an ANSYS calculation is represented in Fig. 12. Conditions for the calculation from a measurement are as follows:

1. Temperature of Cu holder 1 was controlled at 120.088 K;
2. Heat of 3.47 mW was applied by Heater 2;
3. Temperature difference of 0.136 K was measured by two Cernox® sensors.

To reproduce the experiment, the thermal conductivity of the mixture of Cu powder and grease must be 0.775 W/m-K. Figure 13 shows the thermal conductivities of the mixture of Cu powder and grease estimated by ANSYS calculations. It seems that the thermal conductivity gradually increases from 250 to 40 K and then rapidly decreases as the temperature lowers. On the assumption that the mixture of Cu powder and grease is a composite material, the thermal conductivity should monotonically decrease as temperature decreases, according to reference 15. Our estimation is inconsistent with the experimental results of reference 15. Taking the inflection point at around 40 K into consideration, a substantial amount of Cu particles in the mixture must directly contact both surfaces of the Cu holder and Yb:YAG ceramics block. Measurement of the thermal conductivity of the mixture of Cu powder and grease is a hard task, because the mixture of Cu powder and grease is not solid. By using a block of a standard material such as stainless steel, instead of the Yb:YAG ceramics, the estimate by ANSYS calculations might clarify the thermal conductivity of the mixture of Cu powder and grease with high accuracy.

On the other hand, the mixture of Cu powder and grease can be assumed to be a composite material. According to reference 15, the thermal conductivity of epoxy-resin/metal-powder composite materials above 20 K can be calculated by

$$K_c = K_m \cdot \frac{(A - 2V_f + 0.409BV_f^{7/3} - 2.133CV_f^{10/3})}{(A + V_f + 0.409BV_f^{7/3} - 0.906CV_f^{10/3})}, \quad (4)$$

with $A = (2 + K_d)/(1 - K_d)$, $B = (6 + 3K_d)/(4 + 3K_d)$, $C = (3 - 3K_d)/(4 + 3K_d)$ and $K_d = K_f/K_m$. K_c, K_m and K_f are the thermal conductivities of the composite, matrix and filler, respectively. V_f is defined as the volume of filler divided by the volume of the composite. Instead of epoxy-resin and metal-powder, the vacuum grease and Cu powder are assumed to be matrix and filler, respectively, in the equation. We apply values of thermal conductivity: 350 W/m-K from Cryocomp (ver.3.06, Cryodata Inc.) and 0.2 W/m-K [16] of Cu and the Lakeshore vacuum grease at 300 K, respectively. We assume that the vacuum greases from LakeSore Cryogenics Inc. and Rhodia Silicone Italia S.p.A. have the same thermal conductivity. We calculate the thermal conductivity of a vacuum-grease/Cu-powder composite material with V_f of 40%, 45%, and 50%, which results in 0.674 W/m-K, 0.795 W/m-K, and 1.03 W/m-K, respectively. The calculated values are represented in Fig. 13 and are comparable to the estimate from the ANSYS calculations. According to the estimate, V_f of the mixture used in the experiment might be 40 - 45%. Thus, the ANSYS calculation can reproduce the temperature profile along the effective Yb:YAG length and can evaluate the intrinsic thermal conductivity of the Yb:YAG ceramics block, if we have all information on materials and measurements. However, the dependence of the thermal conductivity of the vacuum grease on temperature has not been published. Therefore, we cannot evaluate the thermal con-

ductivity of Yb:YAG ceramics from the CEA Paris-Saclay measurements at this moment. Eventually we established the compensation method for thermal impedances within the CEA Paris-Saclay thermal system.

6. Conclusion

We have conducted a round-robin test of thermal conductivity with three systems at CEA Paris-Saclay and NIFS. Thermal conductivity of 9.8 at% Yb:YAG ceramics was measured from room temperature to a cryogenic environment. We have established a compensation method to evaluate the intrinsic thermal conductivity for each system. Three systems have the ability to evaluate thermal conductivity with high accuracy, in combination with compensation methods for obstacle thermal impedances.

[1] D.J. Ripom, J.R. Ochoa, R.L. Aggarwal and T.Y. Fan, Opt. Lett. **29**, 2154 (2004).
[2] T. Sekine, T. Kurita, M. Kurita, T. Morita, Y. Hatano, Y. Muramatsu, T. Watari, Y. Kabeya, T. Iguchi, R. Yoshimura, Y. Tamaoki, Y. Takeuchi, Y. Mizuta, K. Kawai, Y, Zheng, Y. Kato, T. Suzuki, N. Kurita, T. Kawashima, S. Tokita, J. Kawanaka, N. Ozaki, Y. Hironaka, K. Shigemori, R. Kodama, R. Kuroda and E. Miura, High Energy Density Phys. **36**, 100800 (2020).
[3] K. Tomabechi, Y. Kozaki, T. Norimatsu and Members of Reactor Design Committee, J. Phys. IV France **133**, 791 (2006).
[4] T. Norimatsu, J. Kawanaka, M. Miyanaga, H. Azechi, K. Mima, H. Furukawa, Y. Kozaki and K. Tomabechi, Fusion Sci. Technol. **52**, 893 (2007).
[5] R.L. Aggarwal, D.J. Ripin, J.R. Ochoa and T.Y. Fan, J. Appl. Phys. **98**, 103514 (2005).
[6] J. Lu, H. Yagi, K. Takaichi, T. Uematsu, J.-F. Bisson, Y. Feng, A. Shirakawa, K.-I. Ueda, T. Yanagitani and A.A. Kaminskii, Appl. Phys. B **79**, 25 (2004).
[7] T. Numazawa, O. Arai, Q. Hu and T. Noda, Meas. Sci. Technol. **12**, 2089 (2001).
[8] H. Yagi, T. Yanagitani, T. Numazawa and K. Ueda, Ceram. Int. **33**, 711 (2007).
[9] R. Yasuhara, H. Furuse, A. Iwamoto, J. Kawanaka and T. Yanagitani, Opt. Express **20**, 29531 (2012).
[10] B. Baudouy and A. Four, Cryogenics **60**, 1 (2014).
[11] A. Iwamoto, R. Maekawa and T. Mito, Adv. Cryo. Eng. **49**, 643 (2004).
[12] H. Fujishiro, T. Naito, M. Ikebe and K. Noto, J. Cryo. Super. Soc. Jpn. **28**, 533 (1993) (in Japanese).
[13] C.L. Tsai, H. Weinstock and W.C. Overton, Cryogenics **18**, 562 (1978).
[14] F. Rondeaux, Ph. Bredy and J.M. Rey, Adv. Cryo. Eng. **48**, 197 (2002).
[15] F.F.T. de Araujo and H.M. Rosenberg, J. Phys. D: Appl. Phys. **9**, 665 (1976).
[16] Lake shore Cryogenics, Inc. data sheet.